THE JOURNAL OF BIOLOGICAL CHEMISTRY
Vol. 280, No. 33, Issue of August 19, pp. 29812–29819, 2005

Printed in U.S.A.

Structure and Properties of the C-terminal Domain of Insulin-like Growth Factor-binding Protein-1 Isolated from Human Amniotic Fluid*

Received for publication, April 20, 2005, and in revised form, June 21, 2005
Published, JBC Papers in Press, June 22, 2005, DOI 10.1074/jbc.M504304200

Alberto Sala‡§, Stefano Capaldi§¶, Monica Campagnoli‡, Beniamino Faggion¶, Sara Labò‡, Massimiliano Perduca¶, Assunta Romano‡, Maria E. Carrizo¶, Maurizia Valli‡, Livia Visai‡, Lorenzo Minchiotti‡, Monica Galliano‡‖, and Hugo L. Monaco¶**

From the ‡Department of Biochemistry "A. Castellani," University of Pavia, via Taramelli 3b, 27100 Pavia, Italy and the ¶Biocrystallography Laboratory, Department of Science and Technology, University of Verona, Ca Vignal 1, strada Le Grazie 15, 37134 Verona, Italy

Insulin-like growth factor (IGF)-binding protein-1 (IGFBP-1) regulates the activity of the insulin-like growth factors in early pregnancy and is, thus, thought to play a key role at the fetal-maternal interface. The C-terminal domain of IGFBP-1 and three isoforms of the intact protein were isolated from human amniotic fluid, and sequencing of the four N-terminal polypeptide chains showed them to be highly pure. The addition of both intact IGFBP-1 and its C-terminal fragment to cultured fibroblasts has a similar stimulating effect on cell migration, and therefore, the domain has a biological activity on its own. The three-dimensional structure of the C-terminal domain was determined by x-ray crystallography to 1.8 Å resolution. The fragment folds as a thyroglobulin type I domain and was found to bind the Fe^{2+} ion in the crystals through the only histidine residue present in the polypeptide chain. Iron (II) decreases the binding of intact IGFBP-1 and the C-terminal domain to IGF-II, suggesting that the metal binding site is close to or part of the surface of interaction of the two molecules.

Insulin-like growth factor-binding protein-1 is a member of a family comprising six secreted proteins (designated IGFBP-1[1] to IGFBP-6) that can modulate upon binding the availability and thus the biological effects of insulin-like growth factors I and II (IGF-I and IGF-II). Both inhibition and enhancement of the hormone action have been described, and several mechanisms, including binding of IGFBPs to the extracellular matrix, phosphorylation, and proteolysis, have been shown to modulate their affinity for IGFs. Moreover, an increasing number of reports indicate that IGFBPs can regulate cellular functions independently of their ability to interact with IGFs (1, 2).

Each IGFBP polypeptide chain, ranging in length from 216 to 289 amino acids, may be divided into three distinct domains of approximately equal size. The N- and C-terminal portions exhibit a high primary sequence identity across the six IGFBPs and contain spatially conserved cysteine residues that form intra-domain disulfide bonds. The central domain is the least conserved region and in some of the proteins contains post-translational modifications and proteolytic cleavage sites. On the basis of their sequence homology it is assumed that IGFBPs share a common overall fold and have very similar IGF binding pockets. The N-and C-terminal domains are known to be involved in IGF binding (3), and recently the x-ray structure of the ternary complex of the two domains of IGFBP-4 and IGF-I has been reported (4). In this complex the C-terminal domain was partially disordered, and therefore, a detailed model of this part of the molecule could not be produced. The structure of the N-terminal domain of IGFBP-5, both isolated (NMR data (5)) and complexed to IGF-I (x-ray data (6)), is also known, and NMR spectroscopy has been used to produce a detailed model of the C-terminal domain of IGFBP-6 (7) and to study its interactions with IGF-II (8), but there is no x-ray model available of the C-terminal domain of any member of this protein family, although the C-terminal fragment of IGFBP-4 was crystallized recently (9). Proteolytic cleavage at the mid-region between the two domains of the protein is considered the predominant mechanism for IGF release from all IGFBPs (10), but several studies indicate that the resulting N- and C-terminal fragments still retain the ability to inhibit IGF activity (11). Additionally, recent reports suggest that proteolysis of IGFBPs results in fragments with potential functional properties that differ from those of the intact protein (9, 11).

IGFBP-1 is normally expressed in a tissue-specific manner in the liver, kidney, decidualized endometrium, and luteinizing granulosa cells (12). It is the predominant IGFBP in amniotic fluid (13), a major IGF-binding protein in fetal plasma, and its concentration is increased in maternal circulation during pregnancy. Several studies indicate that the protein plays a relevant role in embryonic growth as a local modulator of IGFs bioavailability at the maternal-fetal interface (14, 15). Moreover, the up-regulation of IGFBP-1 was demonstrated in breast human tumors and was associated with the malignant transformation of breast tissue (16). In addition, IGFBP-1 contains an Arg-Gly-Asp tripeptide that can bind to the recognition site of $\alpha_5\beta_1$ integrin, leading to the stimulation of migration in various cell species (17–20). The mature polypeptide chain of IGFBP-1 is composed of 234 amino acids (the unprocessed precursor is 259 amino acids long) and is phosphorylated at

* This work was supported by grants from the Italian Ministry of Education and Scientific Research (Fondo per gli Investiment della Ricerca di Base and Progetti di Ricerca di Interesse Nazionale).

The atomic coordinates and structure factors (code 1ZT3 and 1ZT5) have been deposited in the Protein Data Bank, Research Collaboratory for Structural Bioinformatics, Rutgers University, New Brunswick, NJ (http://www.rcsb.org/).

§ Both authors contributed equally to this paper.
‖ To whom correspondence may be addressed. Tel.: 39-0382-987-724; Fax: 39-0382-423-108; E-mail: galliano@unipv.it.
** To whom correspondence may be addressed. Tel.: 39-045-8027-903; Fax: 39-045-8027-929; E-mail monaco@sci.univr.it.

[1] The abbreviations used are: IGFBP-1, insulin-like growth factor (IGF)-binding protein-1; ELISA, enzyme-linked immunosorbent assay; PBS, phosphate-buffered saline; SFM, serum-free Dulbecco's modified Eagle's medium; r.m.s.d., root mean square deviation.

three serine residues, 126, 144, and 194 (we will follow the sequence numbering of the unprocessed precursor) (21). Pregnancy-associated proteolysis of several other binding proteins has been described (22), and recent studies have focused on the cleavage of IGFBP-1 by matrix metalloproteases present in amniotic fluid and conditioned medium from decidualized endometrial cells (23, 24)

In this study we describe the isolation of the C-terminal domain of IGFBP-1 from human amniotic fluid and its structural characterization by x-ray crystallography to 1.8 Å resolution. We also show that the C-terminal fragment, which contains the Arg-Gly-Asp tripeptide, retains the capability of the intact protein to stimulate cell migration and that it binds the ferrous ion through the only histidine residue present in the chain.

MATERIALS AND METHODS

Protein Purification and Electrophoretic Analysis—Human amniotic fluid was obtained from discarded amniocentesis samples collected in the weeks 16–18. The pooled fluid (3 liters) was saturated to 90% with ammonium sulfate, and the precipitated proteins, after centrifugation at 10,000 × *g* for 1 h, were dissolved in 50 mM Tris-HCl, pH 8.0, 150 mM NaCl, dialyzed against the same buffer, and fractioned by gel filtration on a 4 × 100-cm Sephadex G100 column. Proteins eluting after the albumin peak were pooled, equilibrated in 6.25 mM Bis-Tris-propane, pH 7.5, and separated on a 2.6 × 30-cm high performance Q-Sepharose column equilibrated with the same buffer (buffer A) and connected to an Åkta Purifier system (Amersham Biosciences). The elution was performed with a 375-min linear gradient from 0 to 100% of 6.25 mM Bis-Tris-propane, pH 9.5, 350 mM NaCl (buffer B) and monitored at 280 nm. The fractions containing the C-terminal fragment of IGFBP-1 were pooled, concentrated, and submitted to gel filtration on a Superdex G75 column (Amersham Biosciences) equilibrated and eluted with 20 mM Tris-HCl buffer, pH 8.0, 150 mM NaCl. Intact IGFBP-1 was isolated by gel filtration on a Superdex G75 column followed by ion exchange chromatography on a Mono Q HR 5/5 column (Amersham Biosciences) equilibrated against 20 mM Tris-HCl, pH 8.0, and resolved with a gradient from 0 to 0.5 M NaCl in the same buffer. The homogeneity of the proteins was checked by SDS-PAGE analysis under reducing and non-reducing conditions and by N-terminal sequence determination in a Hewlett-Packard model G 1000 A sequencer (Centro Grandi Strumenti, University of Pavia). Isoelectric focusing was performed using the immobilized pH gradient system on a laboratory-made polyacrylamide gel cast on GelBond with a non-linear 4–10 pH gradient (25) obtained with acrylamido buffer solutions (Fluka). The pI values were determined by comparison with marker proteins. Analytical polyacrylamide slab gel electrophoresis in the presence of SDS was performed as reported by Laemmli (26) using a Mini PROTEAN II Cell (Bio-Rad). For dephosphorylation 5-μg aliquots of each of the three isoforms of IGFBP-1 and of the C-terminal fragment in 0.05 M Tris HCl, pH 8.5, containing 0.5 mM $MgCl_2$ were exposed to 200 units of alkaline phosphatase (Sigma) at 37 °C for 1 h. The reaction mixtures and samples containing the untreated proteins were diluted 1:1 with the 8 M urea solution containing 0.5% carrier ampholites and submitted to analytical isoelectric focusing.

Antibody Production and Western Blot Analysis—For polyclonal antibody production against IGFBP-1, BALB/c mice were injected intraperitoneally five times at 1-week intervals with 100 μg of the purified IGFBP-1. The antigen was emulsified with an equal volume of complete Freund's adjuvant for the first immunization followed by four injections in incomplete adjuvant. The mice were bled, and the sera were tested for reactivity to the purified IGFBP-1 and its C-terminal fragment using ELISA and Western blot. The specific IgGs were purified by affinity chromatography on protein A-Sepharose columns according to the manufacturer's recommendations (Amersham Biosciences). Antibody titers were assayed either by ELISA or immunoblotting. For Western blot analyses electrophoreses were run on 17% SDS-PAGE, and the proteins were transferred by electroblotting to Immobilon-P polyvinylidene difluoride membranes (Millipore) using a Mini Protean II apparatus (Bio-Rad). The membrane was blocked with 5% w/v skim milk and probed with the mouse antiserum diluted 1:1000. Immunoreactive spots were detected with horseradish peroxidase-conjugated anti-mouse immunoglobulin and developed by the enhanced chemiluminescence method (ECL system, Amersham Biosciences).

Analysis of Cell Migration—Normal human skin fibroblasts (PromoCell Gmbh, Germany) were used for cell culture experiments. Cells were maintained in Dulbecco's modified Eagle's medium supplemented with 10% (v/v) fetal calf serum, 100 units/ml penicillin, 1 mg/ml streptomycin (complete medium) at 37 °C in a 5% CO_2 humidified atmosphere. Purified IGFBP-1 and its C-terminal fragment were dissolved in 0.05 M Tris-HCl, pH 7.4 containing 0.15 M NaCl and diluted with serum-free Dulbecco's modified Eagle's medium at the indicated concentrations. Cells were plated in 35-mm Petri dishes and allowed to grow to confluency. The confluent monolayers were "wounded" by scraping cells in the center of the culture dishes using a rubber policeman to generate an acellular area (27). After repeated rinses with PBS, the monolayers were examined and photographed under an inverted microscope and incubated for 48 h in serum-free Dulbecco's modified Eagle's medium (SFM) with and without 1 μg/ml IGFBP-1 or its C-terminal fragment. At the end of the incubation the cells were fixed in methanol for 15 min at −20 °C, examined, and photographed. The plates were previously marked to ensure that the same area was recorded.

Cell migration was also evaluated in Transwell inserts (8-μm pore size, Nunc, Denmark); 5×10^4 fibroblasts were seeded into the upper wells in 500 μl of SFM alone or with 1 μg/ml IGFBP-1 or its C-terminal fragment. The lower wells contained 500 μl of SFM. Cells were allowed to migrate through the filters for 48 h; non-migrating cells were removed from the upper surface using a cotton swab, and the cells that had migrated to the bottom surface of the inserts were fixed and stained with the Diff-Quick staining kit (Medion Diagnostic GmbH, Switzerland) according to the manufacturer's instructions. Migration was quantified by counting the stained cells in 10 non-overlapping fields using a light microscope fitted with a grid eyepiece. The data are the means ± S.D. of triplicate wells from at least two different protein preparations.

For the 3-(4,5-dimethylthiazol-2-yl)-2,5-diphenyltetrazolium bromide (MTT) assay cells (20,000 cells/well) were plated on 96-well plates and grown for 48 h. 3-(4,5-Dimethylthyazol-2-yl)-2,5 diphenyltetrazolium bromide) (Sigma) was added to 1 mg/ml for 4 h followed by extraction as reported (20).

Production of Recombinant IGF-II—The cDNA coding for mature IGF-II (residues 25–91) was amplified by PCR using specific primers designed to introduce BamHI and HindIII restriction sites and a sequence coding for a thrombin cleavage site at the end of the protein chain. The fragment was digested and ligated in the pQE50 vector (Qiagen), which expresses a C-terminal His_6-tagged fusion protein. *Escherichia coli* BL21 cells, transformed with the IGF-II-pQE50 construct, were grown at 37 °C in LB medium, and protein expression was induced overnight by the addition of 0.5 mM isopropyl 1-thio-β-D-galactopyranoside. The cells were harvested and sonicated. Inclusion bodies containing the recombinant IGF-II were washed twice with 20 mM Tris, pH 7.5, 0.5 M NaCl containing 0.1% Triton X-100, and the protein was solubilized in the same buffer containing 6 M guanidine HCl and 20 mM reduced glutathione. The solution was clarified by centrifugation, and the supernatant was applied to a Ni^{2+}- Sepharose column equilibrated in the same buffer. On-column refolding was carried out with a linear 6–0 M guanidine HCl gradient in 20 mM Tris, pH 7.5, 0.5 M NaCl containing 10 mM imidazole. The recombinant His_6-tagged protein was eluted with a linear 10 mM–0.5 M imidazole gradient. The fractions containing the recombinant IGF-II were collected, concentrated, and further purified by gel filtration chromatography on a Superdex G75 column. The final purity was checked by SDS-PAGE and immunoblotting with an anti-His_6 horseradish peroxidase-conjugated monoclonal antibody (Sigma). The protein was concentrated to 1 mg/ml, dialyzed against saline phosphate buffer (PBS), and stored at - 80 °C.

ELISA Assays—To examine the binding of IGFBP-1 and its C-terminal domain to IGF-II by ELISA, microtiter wells were coated for 90 min at 37 °C with 100 μl of 1 μg/ml IGF-II in 50 mM sodium carbonate, pH 9.5. After washing in PBST (PBS containing 0.1% v/v Tween 20), the wells were blocked at 4 °C overnight with 200 μl of 2% (w/v) bovine serum albumin in PBS. For the binding assay, 1 μg of IGFBP-1 and 0.5 μg of its C-terminal fragment in 100 μl of 0.1 mM sodium acetate, pH 5.0, were added to the coated wells and incubated for 60 min at room temperature.

For the inhibition assay, IGFBP-1 and its C-terminal fragment were incubated for 1 h at room temperature with 100 μM $FeCl_2$ dissolved in 0.1 mM sodium acetate, pH 5.0, before addition to the coated wells. Dose dependence was tested by incubating the intact protein with different concentrations of $FeCl_2$. The plates were then extensively washed with PBST and incubated for 90 min with 1 μg of mouse anti-IGFBP-1 IgG dissolved in PBS with 2% bovine serum albumin. After washing 5 times

with PBST, the microtiter wells were incubated for 1 h with rabbit anti-mouse IgG conjugated to horseradish peroxidase (1:1000 dilution; Dako, Gostrup, Denmark). Finally, the conjugated enzyme was treated with *o*-phenylethylenediamine dihydrochloride (Sigma), and the absorbance at 492 nm was monitored with a micro-plate reader (Bio-Rad).

Crystallization and X-ray Data Collection—Screening for crystallization conditions was performed with the hanging drop method at 4 and 20 °C using Hampton Research Screens and mixing 1 μl of the protein solution and the same volume of precipitating solution and equilibrating *versus* 0.3 ml in the reservoir. Larger diffraction quality crystals could be obtained by using bigger volumes with the sitting drop method. The crystals grow by mixing equal volumes of 35% dioxane, and the protein dissolved in 0.02 M Tris-HCl, pH 7.5, at a concentration of 20 mg/ml. The crystals are orthorhombic, space group $P2_12_12$, with unit cell parameters a = 38.54 Å, b = 60.39 Å, and c = 31.24 Å and contain one C-terminal domain of IGFBP-1 in the asymmetric unit.

The diffraction data were collected from crystals frozen at 100 K after a brief immersion in a mixture of 70% of the mother liquor and 30% glycerol. The data for the native crystals and the two heavy atom derivatives were obtained using copper Kα radiation from a Rigaku RU-300-rotating anode x-ray generator with a Mar345 imaging plate area detector. The data for the co-crystal with $FeSO_4$ were collected at the XRD1 beamline of the Elettra synchrotron in Trieste (λ = 1.00 Å). The two heavy atom derivatives were prepared by overnight soaking of a crystal in mother liquor with the addition of the two compounds at a final concentration of about 1 mM. The data were indexed, integrated, and reduced using the programs MOSFLM (28) and AUTOMAR and Scala (29). The diffraction data statistics are summarized in Table I.

Structure Determination and Refinement—Initial phases to 2.3 Å resolution were determined by multiple isomorphous replacement with the two heavy atom derivatives. The two platinum sites were located in a difference Patterson map (30) and refined using the program MLPHARE (29). The single isomorphous replacement phases were used to locate the most significant mercury site in the difference Fourier map. These two major sites (one site from each of the two derivatives) were used as input for the program autoSHARP (31) that was used to locate the minor sites of the two derivatives and for density modification and final phasing. The electron density map thus produced was of excellent quality and could be readily interpreted. The initial model was built in the high quality map at 2.3 Å resolution using the program O (32) and was subsequently refined with the program REFMAC (33). During the process of refinement and model building, the quality of the model was controlled with the program PROCHECK (34). Solvent molecules were added to the model in the final stages of refinement according to hydrogen-bond criteria and only if their B factors refined to reasonable values and if they improved the *R*free. The final model contains 642 non-hydrogen protein atoms and has very reasonable geometry (see Table I), with 87.5% of the residues in the most favored regions of the Ramachandran plot and the remaining 12.5% in the additionally allowed region. The iron in the co-crystal was modeled into a difference Fourier map phased by the refined, unliganded structure, and the model was refined with REFMAC using the same criteria followed in the refinement of the apoprotein. The final statistics of the co-crystals are also given in Table I.

RESULTS

Isolation of IGFBP-1 C-terminal Fragment and Intact IGFBP-1 from Human Amniotic Fluid—The purification protocol used in the present work was developed with the aim of isolating a large number of components from human amniotic fluid. Proteins were thus precipitated with up to 90% ammonium sulfate concentration, and after a preliminary fractionation by gel filtration chromatography, the low molecular mass components were resolved by anion exchange chromatography and further purified by gel filtration (data not shown). The fractions showing the presence of a single band, when checked by SDS gel electrophoresis, were submitted to N-terminal sequence determination. The first 15 residues of a homogeneous 11-kDa polypeptide chain were VTNIKKWKEPCRIEL, and a search in the SWISSPROT data bank revealed that this sequence was identical to an internal amino acid sequence of IGFBP-1 starting from residue 166 (the numbering corresponds to the full-length precursor, SWISSPROT accession number P08833). The apparent molecular mass of the fragment accounts for the entire C-terminal domain (spanning residues 176–259) and the last portion of the central domain (residues 166–175). The recovery of the fragment was estimated in 1.5 mg/liter of amniotic fluid, using the extinction coefficient calculated from the amino acid composition. Three components showing an apparent molecular mass of 30 kDa were identified as isoforms of the intact IGFBP-1 on the basis of their unique N-terminal sequence, APWQCAPCSAEKLAL (residues 26–40 in the SWISSPROT numbering). It is known that during pregnancy decidual cells produce the non-phosphorylated as well as the differently phosphorylated IGFBP-1 forms characteristic of human pregnancy plasma (23, 35). The anion exchange chromatography retention times of the isoforms correlate with their more acidic pI values, and both acquire the same net charge of the non-phosphorylated protein after treatment with alkaline phosphatase. These results show that the IGFBP-1 isoforms present in human amniotic fluid are differently phosphorylated forms of the protein. The C-terminal fragment was submitted to analytic isoelectric focusing before and after the alkaline phosphatase treatment, and its mobility shift upon removal of the phosphate group revealed that it is phosphorylated as well. The pI values measured for the unmodified intact protein and its C-terminal fragment were 5.2 and 7.2, respectively, in agreement with the theoretical values calculated on the basis of their amino acid composition. The intact IGFBP-1 was used to produce polyclonal antibodies in mouse that were found to react with both the intact protein and the C-terminal region. A fresh sample of amniotic fluid was then resolved by SDS gel electrophoresis and, after electroblotting, probed with the anti-IGFBP-1 antibodies that recognized a single band corresponding to the molecular mass of the intact protein. This result shows that the cleavage producing the C-terminal fragment occurred in the amniotic fluid either during the long-term storage or during the purification procedure. Although the isolation of the C-terminal portion of IGFBP-1 from a natural source has not been reported before, amniotic fluid is known to contain several proteases belonging to different classes that can cleave IGFBPs.

The IGFBP-1 C-terminal Fragment Promotes Cell Migration—IGFBP-1 stimulates cell migration in an IGF-independent manner through the binding of its RGD motif to $\alpha_5\beta_1$ integrin (17, 18, 19). Because the C-terminal fragment contains the RGD sequence, its possible effect on cell migration was evaluated. In these experiments human fibroblasts were used because of their ability to migrate in response to different stimuli and because they do not express IGFBP-1 as verified by immunoblotting of concentrated conditioned medium (data not shown). Migration was assessed by the ability of cells to move into an empty area created by a rubber policeman. The cells, after wounds, were allowed to grow for 48 h in SFM containing 1 μg/ml IGFBP-1 or its C-terminal fragment, and images were taken at 0 and 48 h. Fig. 1*A* shows that in the control plate the cells grow to almost confluency slightly beyond the wounding line, whereas fibroblasts incubated with both the intact protein and the C-terminal fragment are still sparse but have migrated in the denuded area far beyond the wounding line.

Cell migration was confirmed and quantified in a Transwell system using the same protein concentrations and incubation time as in the wounding assay. IGFBP-1 and the C-terminal fragment showed, respectively, a 233 ± 26 and 186 ± 27% increase over the control of the cells migrated to the underside of the filters. The percentage of migrating cells as the average of triplicate wells from different protein preparations is reported in Fig. 1*B*.

IGFBP-1 or the C-terminal fragment does not significantly affect cell proliferation as evaluated using 3-(4,5-dimethylthiazol-2-yl)-2,5-diphenyltetrazolium bromide as a marker of cellu-

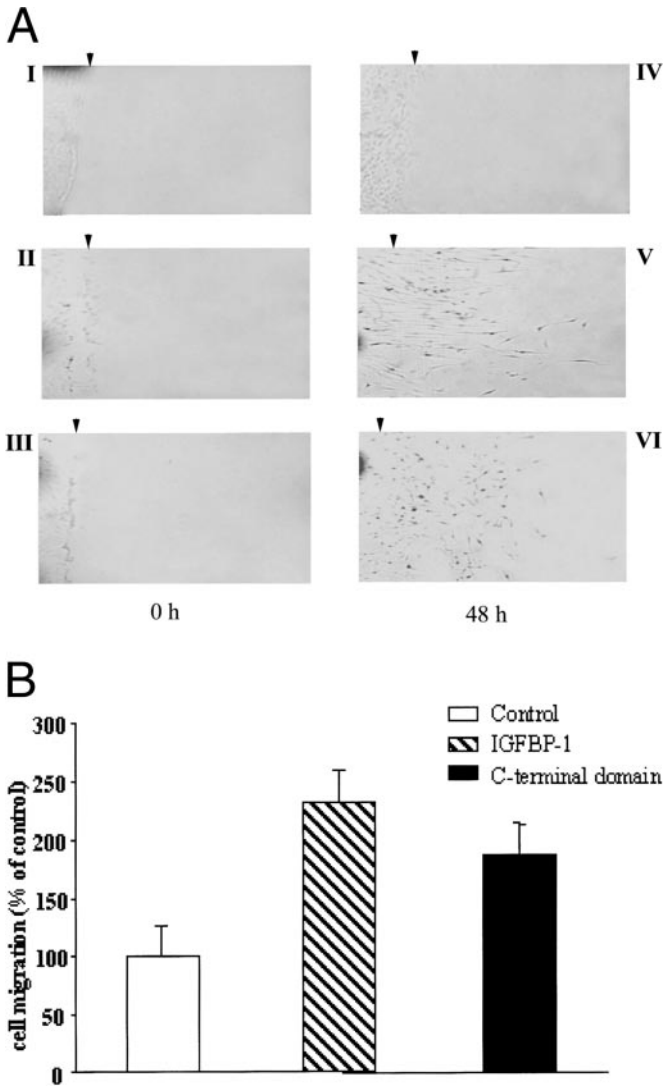

FIG. 1. **IGFBP-1 and its C-terminal fragment induce cell migration.** *A*, confluent fibroblast cells were wounded with a rubber policeman (time 0 h *panels I–III*) and allowed to migrate into the denuded area for 48 h (time 48 h *panels IV–VI*) in either SFM alone (*panel IV*) or containing 1 μg/ml IGFBP-1 (*panel V*) or 1 μg/ml C-terminal fragment (*panel VI*). The *dark spot* on the left side of each photograph marked the Petri dishes to ensure that the same area was recorded. The *arrowheads* indicate the wound edge. *B*, 5×10^4 fibroblasts were seeded into the upper wells of Transwell inserts (8-μm pore size membrane) and allowed to migrate in the presence of either SFM alone or with 1 μg/ml IGFBP-1 or its C-terminal fragment for 48 h. Migrated cells to the underside of the membranes were stained with Diff-Quick and visually counted. The *graph* represents the mean ± S.D. of triplicate wells from at least two different protein preparations

larity after a 48 h culture (data not shown), and therefore, the cell migration observed is not a secondary effect of cell proliferation. These results show that the C-terminal fragment of IGFBP-1 can stimulate cell migration and, therefore, that it retains the effect of the intact protein.

X-ray Structure of the C-terminal Fragment of IGFBP-1—The 2.3 Å experimentally phased map did not show electron density for the first 6 amino acids of the polypeptide chain and for the last 8 amino acids. The polypeptide chain was built starting with Trp-172 up to Cys-251. The side chains of the first two amino acids (Trp-172 and Lys-173) were not well defined in the maps. The final model, refined to 1.8 Å resolution, corresponds to 80 amino acids, 642 protein atoms, 1 dioxane molecule, and 42 water molecules. The conventional R factor is 22.4%, and the free R factor, calculated with 10% of the reflections, is 27.5% (Table I). The R factors and r.m.s.d. values of Table I were calculated with the program REFMAC (33). The stereochemical quality of the protein model was assessed with the program PROCHECK (34); 87.5% of the residues are in the most favorable region of the Ramachandran plot, and the remaining 12.5% are in the additionally allowed region.

The first element of secondary structure of the domain is a β-turn spanning residues 172–175, the second is an α-helix, which spans 19 residues, from Pro-175 to Thr-193. The next 4 residues in the sequence, Ser-194, Gly-195, Asp-196, and Asp-197, are disordered in the maps. Ser-194 was phosphorylated in the protein used to prepare the crystals that were used in all the x-ray diffraction experiments, but no clear electron density for the phosphate group was present in the maps. The rest of the domain contains four very short strands of anti-parallel β-sheet and 5 additional β turns. The 4 strands span the following residues: 200–201, 219–220, 215–217, and 228–230. A total of 10 residues are, thus, found in β strands, and 24 are found in the 6 β turns. A γ turn of the inverse type is formed by residues Ile-245–Arg-246–Gly-247, where 2 of the 3 residues are part of the RGD motif that binds to integrins. The three disulfide bridges are formed by Cys-176 and Cys-206, by Cys-217 and Cys-228, and by Cys-230 and Cys-251, the last residue that is clearly defined in the maps (36). The electron density of the three bridges is very clear in all the maps.

Fig. 2*A* is a schematic representation of the C-terminal domain of IGFBP-1. The α-helix is *light blue*, and the four short strands of β structure are represented as *arrows*. The three disulfide bridges and the phosphorylated serine (Ser-194) are also represented in the figure. Notice the position of the RGD motif (Arg-246–Gly-247–Asp-248), represented in the figure as *ball and stick models*, on the opposite side of the α-helix. The figure shows also the position of the Fe^{2+} binding site (see next paragraph). Fig. 2*B* is a stereoview of the Cα chain trace of the molecule in approximately the same orientation.

The IGFBP-1 C-terminal Fragment Binds the Ferrous Ion—Crystals of the C-terminal domain of IGFBP-1 were soaked in 10 mM solutions of the following metal compounds: $CaCl_2$, $FeSO_4$, $FeCl_3$, $CoCl_2$, $NiSO_4$, and $MnCl_2$. X-ray data were collected, and difference Fourier maps were calculated and examined. The crystals soaked in $FeCl_3$ were found not to diffract at all, whereas the crystals soaked in the other metals did not show any significant extra electron density with only one exception, $FeSO_4$, which presented a very high peak clearly visible with a cutoff of 7 σ in the $F_{obs} - F_c$ map and present in a position of the molecule where it could be easily interpreted in chemical terms. Fig. 3 shows the electron density of the Fe^{2+} ion in the co-crystals of the C-terminal domain of IGFBP-1 in both an $F_{obs} - F_c$ and a $2F_{obs} - F_c$ maps. The red density of the $F_{obs} - F_c$ map is contoured at a 7-σ level, and the blue electron density of the $2F_{obs} - F_c$ map is contoured at a 1.5-σ level. The *diagram* on the *right hand* of the figure represents the species coordinated to the bivalent ion. The Fe^{2+} ion is coordinated tetrahedral to a nitrogen of the ring of the only histidine present in the polypeptide chain, His-213, and to the oxygen of the side chain of Ser-214. The other two positions are occupied by 2 water molecules that are also bound to the polypeptide chain nitrogens of residues 207 and 215. Of the 4 coordination positions 2 involve side chains, those of His-213 and Ser-214, whereas the other two are dependent on two polypeptide chain nitrogens.

Iron (II) Reduces the Binding of IGFBP-1 and Its C-terminal Domain to IGF-II—The hypothesis that the binding of intact IGFBP-1 and its C-terminal domain to IGF-II, the major growth factor in amniotic fluid, might be affected by the presence of ferrous ion was tested by using an ELISA assay. The

TABLE I
Crystal structure determination statistics

The values in parentheses refer to the highest resolution shell, *i.e.* for the data collected 1.90–1.80 Å for the native data set, 2.42–2.30 Å for the heavy atom derivatives, and 1.88–1.82 for the co-crystal with Fe(II). The highest resolution shells used in the refinements are 1.90–1.80 Å for the apoprotein and 1.88–1.82 Å for the co-crystals with $FeSO_4$.

Data set	Native	K_2PtCl_4	$C_2H_5HgOHPO_2$	Native + $FeSO_4$
Space group	$P2_12_12$	$P2_12_12$	$P2_12_12$	$P2_12_12$
a (Å)	38.54	38.92	38.63	38.21
b (Å)	60.39	60.40	60.71	59.60
c (Å)	31.24	31.42	31.40	31.06
Resolution range (Å)	20.1-1.8	32.7-2.3	32.6-2.3	32.1-1.8
Observed reflections	44,453	12,950	24,374	23,571
Independent reflections	7,168	3,557	3,580	6,773
*R*sym (%)	4.1 (27.4)	6.8 (29.4)	6.7 (17.3)	4.4 (8.5)
I/σ	14.2 (2.8)	9.0 (3.4)	10.7 (4.4)	8.9 (5.6)
Completeness (%)	99.5 (98.1)	99.5 (99.5)	99.9 (99.2)	97.0 (98.3)
Sites		2	2	
*R*cullis (acentric/centric)		0.718/0.696	0.682/0.622	
Phasing power (acentric/centric)		1.331/1.275	1.519/1.627	
Reflections in refinement	6,801			6,267
*R*cryst (%)	22.36 (32.1)			21.64 (22.8)
*R*free (%) (test set 10%)	27.50 (27.4)			27.18 (43.3)
Protein atoms	642			642
Water molecules	42			61
r.m.s.d. on bond lengths (Å)	0.008			0.010
r.m.s.d. on bond angles (°)	1.082			1.570
Planar groups (Å)	0.004			0.005
Chiral volume deviation ($Å^3$)	0.073			0.086
Average B factor ($Å^2$)	23.59			24.30
Protein atoms	23.19			23.42
Solvent atoms	29.74			33.06

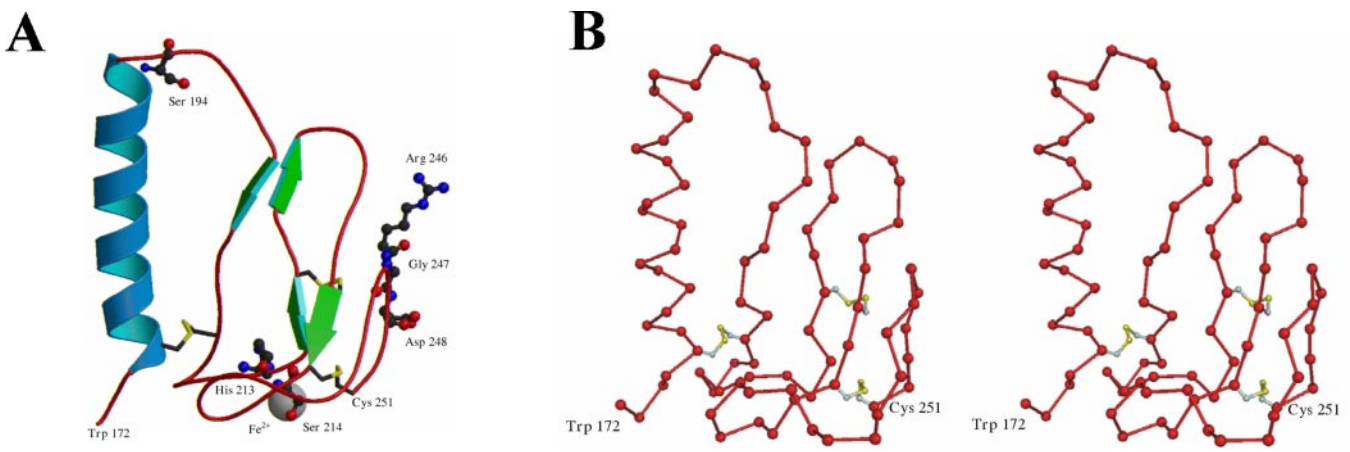

FIG. 2. **Overall structure and folding of the C-terminal domain of IGFBP-1.** *A*, *ribbon representation* of the C-terminal domain of IGFBP-1. The α- helix is *light blue*, the four short strands of β structure are *green*, and coil is *red*. The three disulfide bridges are shown in *yellow*. The diagram shows the phosphorylated serine (Ser-194, disordered in the electron density maps), and the RGD motif (Arg-246–Gly-247–Asp-248) as *ball and stick models*. The Fe^{2+} ion is represented as a *gray sphere*. The figure was prepared using the program MOLSCRIPT (49). *B*, stereoview of the Cα chain trace of the domain in approximately the same orientation. This figure was prepared using Dino (www.dino3d.org).

assays were performed in sodium acetate buffer instead of PBS to avoid the precipitation of ferrous phosphate and to maintain a slight acidic pH, which prevents oxidation of the metal ion. The binding experiments showed that the intact protein binds to IGF-II with higher affinity when compared with the C-terminal domain, a result in agreement with the data reported for other IGFBPs (4). In addition, incubation with ferrous ion reduced the binding of both intact IGFBP-1 and its C-terminal fragment with the growth factor, and this inhibition process was abolished by the addition of EDTA (Fig. 4*A*). The inhibition curve was determined by incubating the intact protein with increasing amounts of ferrous chloride, and the fitting shown in Fig. 4*B* was obtained assuming that the effect of the ferrous ion is competitive. A similar analysis was not performed with the C-terminal fragment because of its lower affinity for IGF-II. These results suggest that the residues involved in the binding to the ferrous ion are in a region of IGFBP-1 at or near the area of interaction with IGF-II.

DISCUSSION

This work describes the structural properties of the C-terminal domain of IGFBP-1 and shows that it maintains the effect of the intact protein on cell motility. The fragment was isolated from human amniotic fluid by conventional chromatographic procedures, and our results indicate that the degradation of IGFBP-1 occurred during the storage or the processing of the fluid that, when examined immediately after sample collection, contains only the intact protein. The polypeptide chain has a unique N-terminal sequence, and therefore, it originates from a specific proteolytic cleavage of the entire protein. IGFBP proteolysis is a well recognized mechanism that controls IGF bioavailability and, although little is known about the susceptibility of IGFBP-1 to enzymatic cleavage *in vivo*, the protein has been recognized as a potential physiological substrate for matrix metalloproteases (24) such as MMP-11 (stromelysin-3) (37) and MMP-26 (matrilysin 2) (38). Both enzymes cleave *in vitro*

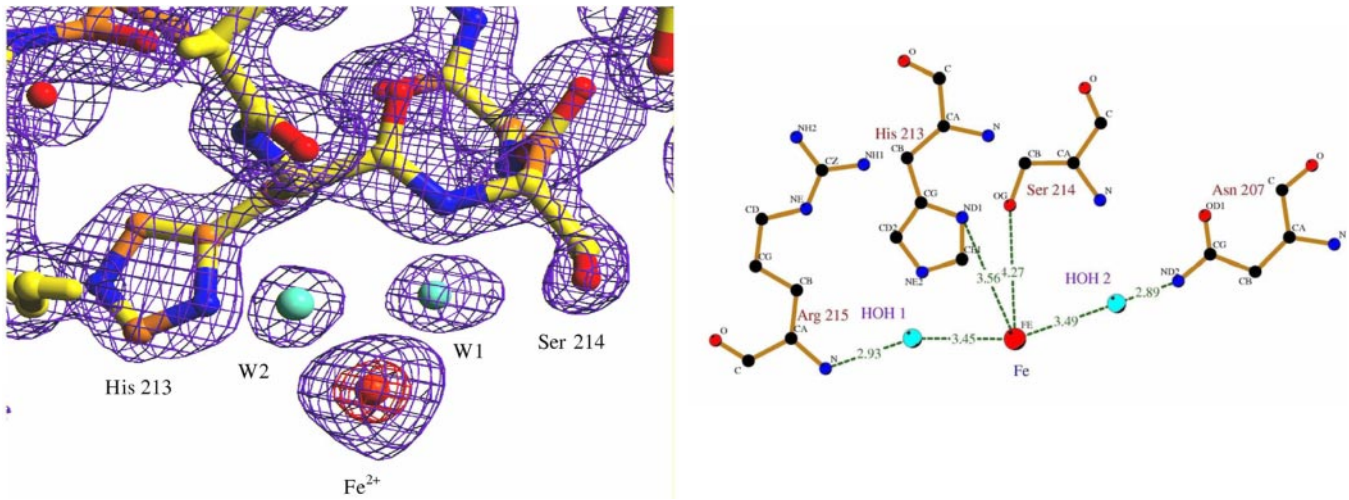

FIG. 3. **Iron ion binding to the C-terminal domain of IGFBP-1.** *Left*, electron density of the Fe^{2+} ion in the co-crystals of the C-terminal domain of IGFBP-1. The *red density* of the $F_{obs} - F_c$ map is contoured at a 7-σ level, the *blue electron density* of the $2F_{obs} - F_c$ map is contoured at a 1.5-σ level. The figure was prepared using the programs XtalView (50) and Raster3D (51). The *right diagram*, representing the groups coordinated to the Fe^{2+} ion, was prepared using the program LIGPLOT (52).

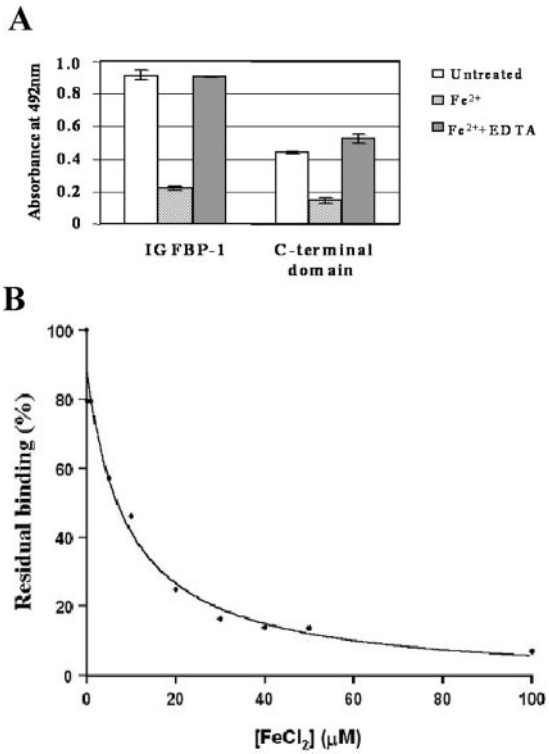

FIG. 4. **Inhibition of IGFBP-1 and of its C-terminal domain binding to IGF-II induced by ferrous ions.** *A*, binding of intact IGFBP-1 and its C-terminal fragment to IGF-II by ELISA. The inhibition was assessed after preincubating the protein with 100 μM $FeCl_2$; the addition of 100 μM EDTA restores the binding. The data shown represent the means and S.D. from duplicated ELISA assays and are representative of two separate experiments. The *y* axis shows the absorbance at 492 nm determined with a micro-plate reader. *B*, inhibition of IGFBP-1 binding to IGF-II determined by ELISA. The protein was preincubated with increasing amounts of $FeCl_2$, and the *y* axis shows the residual binding. The binding of IGFBP-1 to IGF-II in the absence of ferrous ion was set equal to 100%. The fit was obtained considering the process induced by the metal competitive and represents the duplicated mean and S.D. of two independent measurements.

the polypeptide chain of IGFBP-1 between His-165 and Val-166, thus producing a fragment with the same N-terminal sequence that we have found. The observation that the fragment represents a major component of the fluid whereas only small amounts of intact IGFBP-1 are obtained can be ascribed to long term storage of the amniotic fluid in the absence of protease inhibitors. The lack of comparable amounts of the 16-kDa N-terminal domain is likely due to the intrinsic instability of this portion of the molecule. On the contrary, the stability of the C-terminal region suggests that it is a completely very well structured domain of the whole protein, a property that has also been reported for other IGFBPs (11) and is confirmed by our x-ray diffraction studies.

IGFBP-1 stimulates cell migration, and several reports have established that this effect is caused by the binding of its RGD motif to the specific domain of $\alpha_5\beta_1$ integrin present on cell surfaces and have suggested that this interaction results in an intracellular signaling event (20). The requirement of this sequence for a migration promoting effect, initially shown with Chinese hamster ovary (18) and vascular smooth muscle cells (19), has also been demonstrated for placental trophoblast cells (20). In all these models, however, it is clear that not only an intact RGD motif but also some other regions of IGFBP-1 are necessary for binding. Our results indicate that the stable C-terminal domain has the same effect on cell motility as the intact molecule and suggest that proteolytic cleavage of the protein yielding a polypeptide chain with a biological activity on its own might be relevant for the regulatory role of IGFBP-1 on trophoblast migration and invasion.

The C-terminal domain of all the IGFBPs has been recognized on the basis of the disulfide bonding pattern (36) as a member of the thyroglobulin type-I domain (39), which is found in a number of proteins with very diverse function and in different organisms (40, 41). The thyroglobulin type I-fold was first described in the major histocompatibility complex class II-associated p41 Ii fragments bound to cathepsin L (42). More recently, the structure of the C-terminal domain of IGFBP-6 was determined by NMR spectroscopy (7).

The most important element of secondary structure of the C-terminal domain of IGFBP-1 is, as in the other thyroglobulin domains, an α-helix, which in this case spans residues 175–193, *i.e.* it is somewhat longer than in the other two proteins. The α-helix of the p41 Ii fragment is 9 amino acids long (Thr-195—His-203), and that of the C-terminal domain of IGFBP-6 is 15 amino acids long (Pro-162—Thr-176). Using the program LSQKAB (43), we have superimposed the two sets of coordinates of these thyroglobulin domains (PDB entry codes 1ICF and 1RMJ) to the coordinates of the C-terminal domain of IGFBP-1. Fig. 5*A* is a stereo diagram that shows the three protein

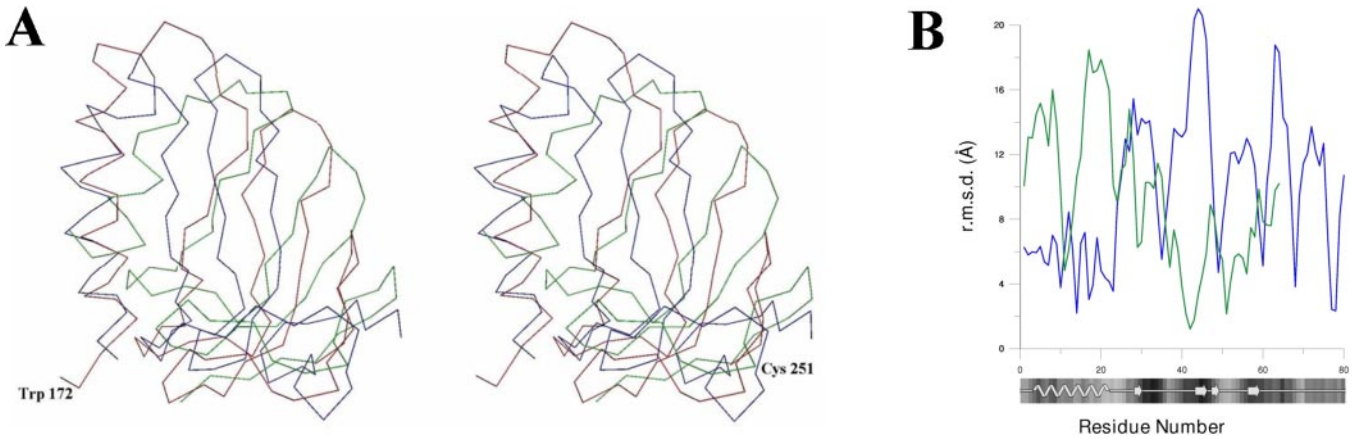

FIG. 5. **Comparison of the C-terminal domain of IGFBP-1 model and two related structures.** *A*, stereo diagram of the three models. The coordinates were superimposed by using the program LSQKAB (43). The model of C-IGFBP-1 is represented in *red* in the figure. The other two structures are (*a*) The NMR structure of C-IGFBP-6, represented in *blue* (Ref. 7, PDB code 1RMJ; the coordinates used for the NMR structure were the first set listed in the PDB file, and the first 27 amino acids were removed from the file) and (*b*) the x-ray structure of the human major histocompatibility complex class II-associated p41 Ii fragment represented in *green* (Ref. 42, PDB code 1ICF). *B*, r.m.s.d. between α-carbon atoms (in Å) of the NMR structure of the C-terminal domain of IGFBP-6 (*blue*), the x-ray structure of the human major histocompatibility complex class II-associated p41 Ii fragment (*green*), and the model of the C-terminal domain of IGFBP-1.

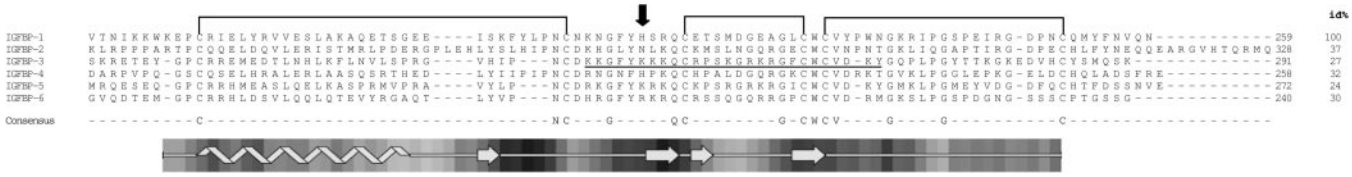

FIG. 6. **Sequence comparison of the C-terminal domain of IGFBP-1 and the other 5 members of the human IGFBP family.** The six sequences of the entire proteins were aligned using the program ClustalW (47), but only the C-terminal domains are represented in the figure. The *column* on the *right hand* gives the identity percentage of each sequence in the figure and that of the C-terminal domain of IGFBP-1; the disulfide bridges are indicated only for IGFBP-1. The *last line* has the amino acids identical in all the C-terminal domains of the group, whereas the *bottom strip* represents the elements of secondary structure of IGFBP-1. An *arrow* indicates the position of His-213, and the metal binding domain of IGFBP-3 is *underlined* and in *bold*.

structures superimposed. Notice that although the essential features of the thyroglobulin type-I domain are preserved in the three models, there is a significant variability in some details like for example the α-helix length and the exact position of the loops defined by the disulfide bonds. The r.m.s.d. in Å of the equivalent α carbons of these two structures and the C-terminal domain of IGFBP-1 are represented in Fig. 5*B* as a function of the amino acid position using the numbering of IGFBP-1.

Ferrous and other divalent ions, Ni^{2+}, Co^{2+}, Zn^{2+}, Mg^{2+}, and Mn^{2+} were found to bind to the C-terminal domain of IGFBP-3, and a 14-amino acid-long metal binding synthetic polypeptide was shown to trigger apoptotic effects as efficiently as intact IGFBP-3 (44). In addition, IGFBP-3 was found to interact with high affinity with the iron-binding proteins transferrin (45) and lactoferrin (46). The hypothesis that the C-terminal domain of IGFBP-1 might bind metal ions as well was tested by immersing crystals of the fragment in sufficiently concentrated solutions of the metals. A total of six ions were tested: Fe^{2+}, Fe^{3+}, Ni^{2+}, Co^{2+}, Ca^{2+}, and Mn^{2+}. Ferric ion was found to completely abolish the diffraction pattern of the crystals, whereas ferrous ion was found to bind in a single very well defined position. Fig. 6 shows the sequences of the C-terminal domains of the six IGFBPs aligned using the program ClustalW (47). The position of His-213 is indicated in the figure with an *arrow*, and the sequence of the metal binding domain of IGFBP-3 is in *bold* and *underlined*. Notice that the domain contains the amino acids aligned with those identified by us as relevant for the binding of Fe^{2+} to the C-terminal domain of IGFBP-1, and therefore, it may be suggested that metal binding in the two proteins could involve equivalent amino acids. The relevant histidine is present only in IGFBP-4, but there is no equivalent to Ser-214 in any of the other members of this protein family, and there is currently no evidence supporting the binding of IGFBP-4 to any metal ion.

On the basis of sequence homology with other IGFBPs, the residues of the IGFBP-1 C-terminal domain that bind the iron ion are located in the region of the protein involved in the binding to IGFs. Photoaffinity-labeling experiments with IGFBP-2 have identified as belonging to the IGF binding site amino acid residues 212–227 but also amino acid residues 266–287 (48). The latter contain Asn-271, which is in a position equivalent to that of His-213 in IGFBP-1 (see Fig. 6). Therefore, our observation that iron (II) reduces the binding of intact IGFBP-1 and of its C-terminal domain to IGF-II is in agreement with a model proposed for another member of this protein family. The fact that metal binding to full-length IGFBP-3 is also inhibited by the presence of IGF-I (44) gives further support to this proposal, but the exact physiological role of metal binding to these proteins will undoubtedly require further work. Taken together, our results indicate that the regulatory action of IGFBP-1 on IGFs and on their functions is more complex than perceived and may involve aspects that had not been identified so far.

Acknowledgments—We thank the staff of Sincrotrone Elettra for assistance during data collection, Rossella Greco, Department of General Biology and Medical Genetics, University of Pavia for supplying the amniotic fluid, Patrizia Arcidiaco, Centro Grandi Strumenti, University of Pavia for sequencing, and Angelo Gallanti, Department of Biochemistry, University of Pavia for cell harvesting.

REFERENCES

1. Baxter, R. C. (2000) *Am. J. Physiol. Endocrinol. Metab.* **278,** 967–976
2. Firth, S. M. and Baxter, R. C. (2002) *Endocr. Rev.* **23,** 824–854

3. Clemmons, D. R. (1998) *Mol. Cell. Endocrinol.* **140,** 19–24
4. Siwanowicz, I., Popowicz, G. M., Wisniewska, M., Huber, R., Kuenkele, K. P., Lang, K., Engh, R. A., and Holak, T. A. (2005) *Structure* **13,** 155–167
5. Kalus, W., Zweckstetter, M., Renner, C., Sanchez, Y., Georgescu, J., Grol, M., Demuth, D., Schumacher, R., Dony, C., Lang, K., and Holak, T. A. (1998) *EMBO. J.* **17,** 6558–6572
6. Zeslawski, W., Beisel, H. G., Kamionka, M., Kalus, W., Engh, R. A., Huber, R., Lang, K., and Holak, T. A. (2001) *EMBO J.* **20,** 3638–3644
7. Headey, S. J., Keizer, D. W., Yao, S., Brasier, G., Kantharidis, P., Bach, L. A., and Norton, R. S. (2004) *Mol. Endocrinol.* **18,** 2740–2750
8. Yao, S., Headey, S. J., Keizer, D. W., Bach, L. A., and Norton, R. S. (2004) *Biochemistry* **43,** 11187–11195
9. Fernandez-Tornero, C., Lozano, R. M., Rivas, G., Jimenez, M. A., Standker, L., Diaz-Gonzalez, D., Forssmann, W. G., Cuevas, P., Romero, A., and Gimenez-Gallego, G. (2005) *J. Biol. Chem.* **280,** 18899–18907
10. Bunn, R. C. and Fowlkes, J. L. (2003) *Trends Endocrinol. Metab.* **14,** 176–181
11. Mark, S., Kubler, B., Honing, S., Oesterreicher, S., John, H., Braulke, T., Forssmann, W. G., and Standker, L. (2005) *Biochemistry* **44,** 3644–3652
12. Lee, P. D., Giudice, L. C., Conover, C. A., and Powell, D. R. (1997) *Proc. Soc. Exp. Biol. Med.* **216,** 319–357
13. Drop. S. L., Kortleve, D. J., and Guyda, H. J. (1984) *J. Clin. Endocrinol. Metab.* **59,** 899–907
14. Han, V. K., Bassett, N., Walton, J., and Challis, J. R. (1996) *J. Clin. Endocrinol. Metab.* **81,** 2680–2693
15. Kajimura, S., Aida, K., and Duan, C. (2005) *Proc. Natl. Acad. Sci. U. S. A.* **102,** 1240–1245
16. Pekonen, F., Nyman, T., Ilvesmaki, V., and Partanen, S. (1992) *Cancer Res.* **52,** 5204–5207
17. Irving, J. A. and Lala, P. K. (1995) *Exp. Cell Res.* **217,** 419–427
18. Jones, J. I., Gockerman, A., Busby, W. H., Jr., Wright, G., and Clemmons, D. R. (1993) *Proc. Natl. Acad. Sci. U. S. A.* **90,** 10553–10557
19. Gockerman, A., Prevette, T., Jones, J. I., and Clemmons, D. R. (1995) *Endocrinology* **136,** 4168–4173
20. Gleeson, L. M., Chakraborty, C., McKinnon, T., and Lala, P. K. (2001) *J. Clin. Endocrinol. Metab.* **86,** 2484–2493
21. Jones, J. I., Busby, W. H., Jr., Wright, G., Smith, C. E., Kimack, N. M., and Clemmons, D.R. (1993) *J. Biol. Chem.* **268,** 1125–1131
22. Davies, S. C., Holly, J. M., Coulson, V. J., Cotterill, A. M., Abdulla, A. F., Whittaker, P. G., Chard, T., and Wass, J. A. (1991) *Clin. Endocrinol.* **34,** 501–506
23. Gibson, J. M., Aplin, J. D., White, A., and Westwood, M. (2001) *Mol. Hum. Reprod.* **7,** 79–87
24. Coppock, H. A., White, A., Aplin, J. D., and Westwood, M. (2004) *Biol. Reprod.* **71,** 438–443
25. Gianazza, E., Giacon, P., Sahlin, B., and Righetti, P. G. (1985) *Electrophoresis.* **6,** 53–56
26. Laemmli, U. K. (1970) *Nature* **227,** 680–685
27. Chen, P., Gupta, K., and Wells, A. (1994) *J. Cell Biol.* **124,** 547–555
28. Leslie, A. G. W. (1992) *Joint CCP4/ESF-EACMB Newslett. Protein Crystallogr.* **26,** pp. 27–33
29. Collaborative Computational Project Number 4 (1994) *Acta Crystallogr. Sect. D* **50,** 760–767
30. Sheldrick, G. M. (1991) in *Isomorphous Replacement and Anomalous Scattering: Proceedings of the CCP4 Study Weekend, January 25–26, 1991* (Wolf, W., Evans, P. R., and Leslie, A. G. W., eds) pp. 23–28, SERC Daresbury Laboratory, Warrington, UK
31. Bricogne, G., Vonrhein, C., Flensburg, C., Schiltz, M. and Paciorek, W. (2003) *Acta. Crystallogr. D. Biol. Crystallogr.* **59,** 2023–2030
32. Jones, T. A., Zou, J. Y., Cowan, S. W., and Kjeldgaard, M. (1991) *Acta Crystallogr. A* **47,** 110–119
33. Murshudov, G. N., Vagin, A. A., and Dodson, E. J. (1997) *Acta Crystallogr. D. Biol. Crystallogr.* **53,** 240–255
34. Laskowski, R. A., MacArthur, M. W., Moss, D. S., and Thornton, J. M. (1993) *J. Appl. Crystallogr.* **26,** 283–291
35. Westwood, M., Gibson, J. M., Davies, A. J., Young, R. J., and White, A. (1994) *J. Clin. Endocrinol. Metab.* **79,** 1735–1741
36. Forbes, B. E., Turner, D., Hodge, S. J., McNeil, K. A., Forsberg, G., and Wallace, J. C. (1998) *J. Biol. Chem.* **273,** 4647–4652
37. Manes, S., Mira, E., Barbacid, M. M., Cipres, A., Fernandez-Resa, P., Buesa, J. M., Merida, I., Aracil, M., Marquez, G., and Martinez-A, C. (1997) *J. Biol. Chem.* **272,** 25706–25712
38. Park, H. I., Turk, B. E., Gerkema, F. E., Cantley, L. C., and Sang, Q. X. (2002) *J. Biol. Chem.* **277,** 35168–35175
39. Malthiery, Y., and Lissitzky, S. (1987) *Eur. J. Biochem.* **165,** 491–498
40. Molina, F., Bouanani, M., Pau, B., and Granier, C. (1996) *Eur. J. Biochem.* **240,** 125–133
41. Galesa, K., Pain, R., Jongsma, M. A., Turk, V., and Lenarcic, B. (2003) *FEBS Lett.* **539,** 120–124
42. Guncar, G., Pungercic, G., Klemencic, I., Turk, V., and Turk, D. (1999) *EMBO. J.* **18,** 793–803
43. Kabsch, W. (1978) *Acta Crystallogr. A* **32,** 922–923
44. Singh, B., Charkowicz, D., and Mascarenhas, D. (2004) *J. Biol. Chem.* **279,** 477–487
45. Weinzimer, S. A., Gibson, T. B., Collett-Solberg, P. F., Khare, A., Liu, B., and Cohen, P. (2001) *J. Clin. Endocrinol. Metab.* **86,** 1806–1813
46. Baumrucker, C. R., Gibson, C. A., and Schanbacher, F. L. (2003) *Domest. Anim. Endocrinol.* **24,** 287–303
47. Thompson, J. D., Higgins, D. G., and Gibson, T. J. (1994) *Nucleic Acids Res.* **22,** 4673–4680
48. Horney, M. J., Evangelista, C. A., and Rosenzweig, S. A. (2001) *J. Biol. Chem.* **276,** 2880–2889
49. Kraulis, P. J. (1991) *J. Appl. Crystallogr.* **24,** 946–950
50. McRee, D. E. (1999) *J. Struct. Biol.* **125,** 156–165
51. Merritt, E. A., and Bacon, D. J. (1997) *Methods Enzymol.* **277,** 505–524
52. Wallace, A. C., Laskowski, R. A., and Thornton, J. M. (1995) *Protein Eng.* **8,** 127–134

Structure and Properties of the C-terminal Domain of Insulin-like Growth Factor-binding Protein-1 Isolated from Human Amniotic Fluid

Alberto Sala, Stefano Capaldi, Monica Campagnoli, Beniamino Faggion, Sara Labò, Massimiliano Perduca, Assunta Romano, Maria E. Carrizo, Maurizia Valli, Livia Visai, Lorenzo Minchiotti, Monica Galliano and Hugo L. Monaco

J. Biol. Chem. 2005, 280:29812-29819.
doi: 10.1074/jbc.M504304200 originally published online June 22, 2005
